View metadata, citation and similar papers at core.ac.uk
brought to you by CORE
provided by Archivio istituzionale della ricerca - Università di Brescia

Nonclassical storage and retrieval of a multiphoton pulse in cold Rydberg atoms

Xue-Dong Tian,[1,2] Yi-Mou Liu,[1] Qian-Qian Bao,[3] Jin-Hui Wu,[1,*] M. Artoni,[4] and G. C. La Rocca[5]
[1]*Center for Quantum Sciences and School of Physics, Northeast Normal University, Changchun 130024, China*
[2]*College of Physics Science and Technology, Guangxi Normal University, Guilin 541004, China*
[3]*College of Physics, Liaoning University, Shenyang 110036, China*
[4]*Department of Engineering and Information Technology and Istituto Nazionale di Ottica (INO-CNR), Brescia University, 25133 Brescia, Italy*
[5]*Scuola Normale Superiore and CNISM, 56126 Pisa, Italy*

(Received 26 January 2018; published 9 April 2018)

We investigate the storage and retrieval of a multiphoton probe field in cold Rydberg atoms with an effective method based on the superatom model. This probe field is found greatly attenuated in light intensity and two-photon correlation yet suffering little temporal broadening as a result of the partial dipole blockade of Rydberg excitation. In particular, the output field energy exhibits an intriguing saturation effect against the input field energy accompanied by an inhomogeneous nonclassical antibunching feature as a manifestation of the dynamic cooperative optical nonlinearity. Our numerical results are qualitatively consistent with those in a recent experiment and could be extended to pursue quantum information applications of nonclassical light fields.

DOI: 10.1103/PhysRevA.97.043811

I. INTRODUCTION

Rydberg atoms [1] with a very large principal quantum number have exaggerated atomic properties, including strong dipole-dipole interactions and long radiative lifetimes, which constitute the basis for many promising quantum information schemes and interesting quantum many-body effects. Such long-range interactions between atoms in a Rydberg state will cause a so-called blockade effect [2–6] that prohibits the simultaneous Rydberg excitation of two or more atoms in a mesoscopic volume. With this Rydberg blockade effect, significant advances have been achieved in the quantum sciences, e.g., with regard to quantum entanglement [7–10], quantum gates [11–15], and quantum devices [16–22], including single-photon sources, filters, absorbers, switches, transistors, etc.

Many interesting phenomena, such as cooperative optical nonlinearity [23–26], nonlocal light propagation [27], bound states of photons [28–30], and crystallization of atomic lattices [31], have been found when the long-range interaction between Rydberg atoms is combined with a famous quantum interference effect, electromagnetically induced transparency (EIT). Driving an ensemble of Rydberg atoms into the EIT regime also helps to implement nontrivial quantum devices, such as single-photon switches [20], single-photon transistors [21,22], and cooperative nonlinear gratings [32]. Quite recently, important experimental progress has been achieved on light storage and retrieval in EIT media of cold [33–35] or thermal [36] Rydberg atoms. It is found that a multiphoton pulse can be engineered to exhibit such peculiar properties as Rydberg-mediated interactions [33] and two-photon states [37]. However, a satisfactory theoretical method to reproduce relevant experimental results is still lacking, although several methods [38–42] have been proposed to deal with the dynamic propagation of single-photon or few-photon pulses in Rydberg-EIT media.

In this paper, we study the storage and retrieval of a multiphoton probe pulse in a one-dimensional (1D) sample of cold Rydberg atoms in the EIT regime. Our calculations are based on a superatom (SA) model [23], extended here to be applicable also in the case of light propagation dynamics [43]. One main finding is that the output probe pulse exhibits a negligible temporal broadening, while its light intensity and two-photon correlation are severely attenuated. This corresponds to a partial dipole blockade of Rydberg excitation, yielding a rough balance between the nonlinear loss for a two-level absorbing system and the linear loss for a three-level EIT system. Moreover, a nonlinear saturation effect is found between the output and input field energies with an inhomogeneous antibunching effect as a manifestation of the dynamic cooperative optical nonlinearity. Last but not least, an intermediate atomic density and a partial Rydberg blockade are required for attaining a bunch of single photons; otherwise, more or less than one photon will be found in each blockade volume of SAs.

II. MODEL AND METHODS

We consider a 1D sample of cold atoms driven into the three-level ladder configuration as shown in Fig. 1(a) with a ground state $|g\rangle$, an excited state $|e\rangle$, and a Rydberg state $|r\rangle$. The lower transition $|g\rangle \leftrightarrow |e\rangle$ is probed by a quantum field of frequency ω_p and amplitude $\hat{\mathcal{E}}_p(z,t)$, while the upper transition $|e\rangle \leftrightarrow |r\rangle$ is coupled by a classical field of frequency ω_c and amplitude $E_c(t)$. Rabi frequencies (detunings) on the coupling and probe transitions are defined, respectively, as $\Omega_c(t) = E_c(t)\wp_{er}/2\hbar$ ($\Delta_c = \omega_c - \omega_{re}$) and $\hat{\Omega}_p(z,t) = g\hat{\mathcal{E}}_p(z,t)$ ($\Delta_p = \omega_p - \omega_{eg}$), with $g = \wp_{ge}\sqrt{\omega_p/(2\hbar\epsilon_0 V)}$ being the single-photon coupling

*jhwu@nenu.edu.cn

 ©2018 American Physical Society

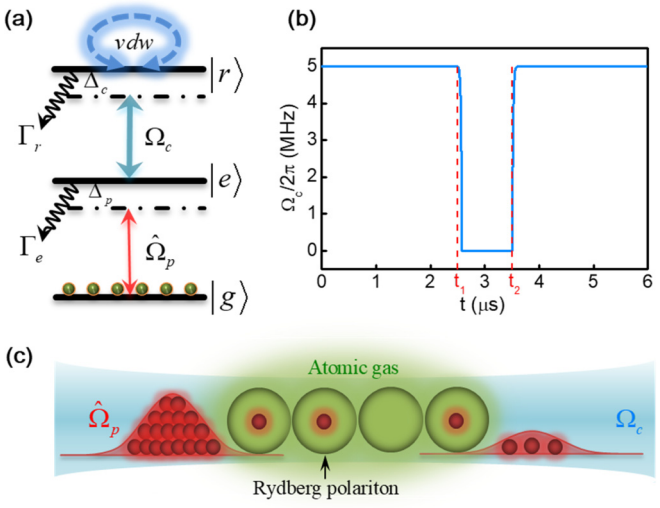

FIG. 1. (a) Level configuration with the lower transition $|g\rangle \leftrightarrow |e\rangle$ probed by a quantum field of Rabi frequency $\hat{\Omega}_p$ and the upper transition $|e\rangle \leftrightarrow |r\rangle$ coupled by a classical field of Rabi frequency Ω_c. vdW denotes the van der Waals interaction experienced by a pair of atoms in the Rydberg state $|r\rangle$. (b) Illustration of a coupling field turned off (on) at time t_1 (t_2) for realizing the storage and retrieval of a probe pulse. (c) Schematic representation of the input and output probe pulses separated by a sample of cold Rydberg atoms envisioned as a collection of superatoms.

strength, V the local quantum volume, $\omega_{re,eg}$ atomic transition frequencies, and $\wp_{er,ge}$ electric dipole moments. In what follows, we will adopt $\hat{P}(z,t) = \sqrt{N}\hat{\sigma}_{ge}(z,t)$ and $\hat{S}(z,t) = \sqrt{N}\hat{\sigma}_{gr}(z,t)$ to describe the slowly varying polarization and spin fields, i.e., the continuum distributions of atomic excitations, with $\hat{\sigma}_{ge} = |g\rangle\langle e|$ and $\hat{\sigma}_{gr} = |g\rangle\langle r|$ being atomic transition operators while N being the atomic volume density. The three optical or atomic fields coupled together satisfy the same time commutation relations $[\hat{\mathcal{E}}_p(z,t), \hat{\mathcal{E}}_p^\dagger(z',t)]/V = [\hat{P}(z,t), \hat{P}^\dagger(z',t)] = [\hat{S}(z,t), \hat{S}^\dagger(z',t)] = \delta(z-z')$ in the limit of very low atomic excitations ($\langle\hat{\sigma}_{gg}\rangle \to 1$).

In a frame rotating with frequencies $\omega_{p,c}$, we can write down the total Hamiltonian $\hat{\mathcal{H}} = \hat{\mathcal{H}}_p + \hat{\mathcal{H}}_{af} + \hat{\mathcal{H}}_{\rm int}$, including the kinetic term $\hat{\mathcal{H}}_p$, the atom-field coupling term $\hat{\mathcal{H}}_{af}$, and the interaction term $\hat{\mathcal{H}}_{\rm int}$:

$$\hat{\mathcal{H}}_p = -\frac{i\hbar c}{V}\int dz \hat{\mathcal{E}}_p^\dagger(z,t)\partial_z\hat{\mathcal{E}}_p(z,t), \tag{1a}$$

$$\begin{aligned}\hat{\mathcal{H}}_{ap} = &-\hbar\int dz[\Delta_p\hat{P}^\dagger(z,t)\hat{P}(z,t)\\ &+(\Delta_p+\Delta_c)\hat{S}^\dagger(z,t)\hat{S}(z,t)]\\ &-\hbar\int dz[g\sqrt{N}\hat{\mathcal{E}}_p^\dagger(z,t)\hat{P}(z,t)\\ &+\Omega_c(t)\hat{S}^\dagger(z,t)\hat{P}(z,t)+\text{H.c.}],\end{aligned} \tag{1b}$$

$$\begin{aligned}\hat{\mathcal{H}}_{\rm int} = &\frac{\hbar}{2}\int dz\int dz'\hat{S}^\dagger(z,t)\hat{S}^\dagger(z',t)\\ &\Delta(z-z')\hat{S}(z',t)\hat{S}(z,t),\end{aligned} \tag{1c}$$

where we have considered that a pair of atoms simultaneously excited to the Rydberg state $|r\rangle$ interact with each other via a van der Waals (vdW) potential $\Delta(z_i - z_j) = C_6/|z_i - z_j|^6$, with z_i and z_j being their positions.

Using Hamiltonian $\hat{\mathcal{H}}$, it is then straightforward to obtain the Heisenberg-Langevin equations:

$$\begin{aligned}\partial_t\hat{P}(z,t) = &-(\gamma_e - i\Delta_p)\hat{P}(z,t)\\ &+i\Omega_c^*(t)\hat{S}(z,t)+i\sqrt{N}\hat{\Omega}_p(z,t),\end{aligned} \tag{2a}$$

$$\begin{aligned}\partial_t\hat{S}(z,t) = &-[\gamma_r - i(\Delta_p+\Delta_c-\langle\hat{\Delta}_s\rangle)]\hat{S}(z,t)\\ &+i\Omega_c(t)\hat{P}(z,t),\end{aligned} \tag{2b}$$

$$\partial_t\hat{\Omega}_p(z,t) = -c\partial_z\hat{\Omega}_p(z,t)+ig^2V\sqrt{N}\hat{P}(z,t), \tag{2c}$$

where $\hat{\Delta}_s = \frac{1}{2}\int dz'\hat{S}^\dagger(z',t)\Delta(z-z')\hat{S}(z',t)$ is the vdW-induced frequency shift while γ_e (γ_r) is the coherence dephasing rate on the transition $|g\rangle \leftrightarrow |e\rangle$ ($|e\rangle \leftrightarrow |r\rangle$). Langevin noises have been omitted here, as it does not affect our calculations in the limits of $\langle\hat{\sigma}_{ee}\rangle \to 0$ and $\langle\hat{\sigma}_{rr}\rangle \to 0$ [40]. To solve these coupled equations, we then introduce the terminology of SA defined as $n_{SA} = NV_{SA}$ atoms in the blockade volume $V_{SA} = 4\pi R_b^3/3$ of radius $R_b \approx [C_6\gamma_e/(|\Omega_c(t)|^2+\gamma_e\gamma_r)]^{1/6}$ [44]. In the mean-field sense, the expected value $\langle\hat{\Delta}_s\rangle$ tends to infinite (vanishing) for the atoms in such SAs with (without) a definite Rydberg excitation, whereas vdW interactions between different SAs are typically very weak and can be qualitatively described by a very small dephasing rate γ_s and a very small frequency shift δ_s [44,45].

With the above considerations, it is clear that the atoms in such SAs with (without) a definite Rydberg excitation behave like a two-level (three-level) system excluding (including) the Rydberg state $|r\rangle$. In the more general case, however, each atom should behave like a superposition of two-level and three-level systems determined solely by the probability of finding a single Rydberg excitation in relevant SAs. That is, the single-Rydberg-excitation probability answers for the interatomic interaction effects in each SA, and a definite (vanishing) Rydberg excitation corresponds to the strongest (weakest) interactions. In this regard, the dynamic equations of polarization and spin fields can be rewritten as

$$\begin{aligned}\partial_t\hat{P}_3(z,t) = &-(\gamma_e - i\Delta_p)\hat{P}_3(z,t)\\ &+i\Omega_c^*(t)\hat{S}_3(z,t)+i\sqrt{N}\hat{\Omega}_p(z,t),\end{aligned} \tag{3a}$$

$$\begin{aligned}\partial_t\hat{S}_3(z,t) = &-[\gamma_r - i(\Delta_p+\Delta_c)]\hat{S}_3(z,t)\\ &+i\Omega_c(t)\hat{P}_3(z,t),\end{aligned} \tag{3b}$$

for the three-level system, and

$$\partial_t\hat{P}_2(z,t) = -(\gamma_e - i\Delta_p)\hat{P}_2(z,t)+i\sqrt{N}\hat{\Omega}_p(z,t) \tag{4}$$

for the two-level system.

To further determine the single-Rydberg-excitation probability answering for the interatomic interaction effects, we then introduce as usual [23] for all relevant SAs the first-order collective states $|G\rangle = |g_1,...g_i,...g_{n_{SA}}\rangle$, $|E^{(1)}\rangle = 1/\sqrt{n_{SA}}\sum_j^{n_{SA}}|g_1,...e_i,...g_{n_{SA}}\rangle$, and $|R^{(1)}\rangle = 1/\sqrt{n_{SA}}\sum_j^{n_{SA}}|g_1,...r_i,...g_{n_{SA}}\rangle$. Other higher-order collective states originating from $|E^{(1)}\rangle$ can be safely neglected if we choose to work near the center of an EIT window where

the excitation to $|E^{(1)}\rangle$ is well suppressed due to quantum destructive interference [26]. Accordingly, we can define $\hat{\Sigma}_{IJ} = |I\rangle\langle J|$ as the collective transition ($I \neq J$) or projection ($I = J$) operators with $\{I,J\} \in \{G,E^{(1)},R^{(1)}\}$, whose dynamic evolution obey the following coupled equations:

$$\begin{aligned}
\partial_t \hat{\Sigma}_{GG}(z,t) &= 2\gamma_e \hat{\Sigma}_{EE}(z,t) - i\sqrt{n_{SA}}\hat{\Omega}_p(z,t)\hat{\Sigma}_{EG}(z,t) \\
&\quad + i\sqrt{n_{SA}}\hat{\Omega}_p^\dagger(z,t)\hat{\Sigma}_{GE}(z,t), \\
\partial_t \hat{\Sigma}_{EE}(z,t) &= -2\gamma_e \hat{\Sigma}_{EE}(z,t) + 2\gamma_r \hat{\Sigma}_{RR}(z,t) \\
&\quad - i[\Omega_c(t)\hat{\Sigma}_{RE}(z,t) - \Omega_c^*(t)\hat{\Sigma}_{ER}(z,t)] \\
&\quad + i\sqrt{n_{SA}}\hat{\Omega}_p(z,t)\hat{\Sigma}_{EG}(z,t) \\
&\quad - i\sqrt{n_{SA}}\hat{\Omega}_p^\dagger(z,t)\hat{\Sigma}_{GE}(z,t), \\
\partial_t \hat{\Sigma}_{GE}(z,t) &= -(\gamma_e - i\Delta_p)\hat{\Sigma}_{GE}(z,t) + i\Omega_c^*(t)\hat{\Sigma}_{GR}(z,t) \\
&\quad - i\sqrt{n_{SA}}\hat{\Omega}_p(z,t)[\hat{\Sigma}_{EE}(z,t) - \hat{\Sigma}_{GG}(z,t)], \\
\partial_t \hat{\Sigma}_{GR}(z,t) &= -(\gamma_r - i\Delta_p - i\Delta_c)\hat{\Sigma}_{GR}(z,t) \\
&\quad + i\Omega_c(t)\hat{\Sigma}_{GE}(z,t) \\
&\quad - i\sqrt{n_{SA}}\hat{\Omega}_p(z,t)\hat{\Sigma}_{ER}(z,t), \\
\partial_t \hat{\Sigma}_{ER}(z,t) &= -(\gamma_e + \gamma_r - i\Delta_c)\hat{\Sigma}_{ER}(z,t) \\
&\quad - i\Omega_c(t)[\hat{\Sigma}_{RR}(z,t) - \hat{\Sigma}_{EE}(z,t)] \\
&\quad - i\sqrt{n_{SA}}\hat{\Omega}_p^\dagger(z,t)\hat{\Sigma}_{GR}(z,t),
\end{aligned} \tag{5}$$

constrained by $\hat{\Sigma}_{GG} + \hat{\Sigma}_{EE} + \hat{\Sigma}_{RR} = 1$ and $\hat{\Sigma}_{IJ} = \hat{\Sigma}_{JI}^\dagger$. These equations are similar to those for atomic transition or projection operators $\hat{\sigma}_{ij}$ with $\{i,j\} \in \{g,e,r\}$, except that $\hat{\Omega}_p(z,t)$ has been replaced by $\sqrt{n_{SA}}\hat{\Omega}_p(z,t)$. In the case of a very large n_{SA}, the Rydberg-excitation probability $\langle\hat{\Sigma}_{RR}\rangle$ in a SA should be much larger than its atomic counterpart $\langle\hat{\sigma}_{rr}\rangle$ so that it is not negligible, even for a very weak probe field. Note, however, that we cannot simply assume $\langle\hat{\Sigma}_{RR}\rangle = n_{SA}\langle\hat{\sigma}_{rr}\rangle$ in the presence of an essential Rydberg blockade effect.

Solving Eqs. (3)–(5) together, it is possible then to attain the conditional probe polarizability

$$\begin{aligned}
\hat{P}(z,t) &= \hat{P}_2(z,t)\langle\hat{\Sigma}_{RR}(z,t)\rangle \\
&\quad + \hat{P}_3(z,t)[1 - \langle\hat{\Sigma}_{RR}(z,t)\rangle],
\end{aligned} \tag{6}$$

with the consideration that (i) $\langle\hat{\Sigma}_{RR}\rangle$ determines how the two-level system and the three-level system interplay as a result of interatomic interactions to yield different light propagation dynamics, and (ii) the two-photon correlation $g_p^{(2)}(z,t) = \frac{\langle\hat{\mathcal{E}}_p^\dagger(z,t)\hat{\mathcal{E}}_p^\dagger(z,t)\hat{\mathcal{E}}_p(z,t)\hat{\mathcal{E}}_p(z,t)\rangle}{\langle\hat{\mathcal{E}}_p^\dagger(z,t)\hat{\mathcal{E}}_p(z,t)\rangle\langle\hat{\mathcal{E}}_p^\dagger(z,t)\hat{\mathcal{E}}_p(z,t)\rangle}$ should be introduced to answer for the modification of photon statistics conditioned upon a Rydberg blockade. That is, we should replace $\hat{\Omega}_p^\dagger(z,t)\hat{\Omega}_p(z,t)$ with $\langle\hat{\Omega}_p^\dagger(z,t)\hat{\Omega}_p(z,t)\rangle g_p^{(2)}(z,t)$ to reserve the two-particle quantum correlation arising from the vdW interaction. Accordingly, Eq. (2), describing the dynamic evolution of a probe pulse, can be divided into the following two coupled equations:

$$\partial_z \Omega_p(z,t) = +i(g^2V/c)\sqrt{N}P(z,t), \tag{7a}$$

$$\begin{aligned}
\partial_z g_p^{(2)}(z,t) &= -2(g^2V/c)\sqrt{N}\Sigma_{RR}(z,t) \\
&\quad \times\left[\frac{P_2(z,t) - P_3(z,t)}{\Omega_p(z,t)}\right] g_p^{(2)}(z,t),
\end{aligned} \tag{7b}$$

where $O(z,t) = \langle\hat{O}(z,t)\rangle$ has been used to represent the expectation value of operator $\hat{O}(z,t)$. We have also considered that (i) $g_p^{(2)}(z,t)$ is only determined by the nonlinear absorption with the linear one excluded and (ii) time derivatives $\partial_t\ldots$ are negligibly small as compared to space derivatives $c\partial_z\ldots$ in the slow-light regime.

III. RESULTS AND DISCUSSION

In this section, we implement numerical calculations by modulating the coupling field [see Fig. 1(b)] to study light storage and retrieval [see Fig. 1(c)] in a Rydberg-EIT medium of length $L = 600\,\mu$m and density $N = 7.5 \times 10^{11}$ cm^{-3}. We assume, in particular, $|g\rangle \equiv |5S_{1/2}, F = 2\rangle$, $|e\rangle \equiv |5P_{3/2}, F = 3\rangle$, and $|r\rangle \equiv |60s_{1/2}\rangle$ for cold ^{87}Rb atoms. Then we have $\gamma_e = 3.0 \times 2\pi$ MHz, $\gamma_r = 2.0 \times 2\pi$ kHz, and $C_6 = 1.4 \times 10^{11} \times 2\pi$ s$^{-1}\,\mu$m^{-1}. In reference to a practical experiment, the one- and two-photon laser linewidths $\delta\omega_{1,2} \simeq (50,100) \times 2\pi$ kHz [23] need to be included in the dephasing rates so that we have $\gamma_e \to \gamma_e + \delta\omega_1$ and $\gamma_r \to \gamma_r + \delta\omega_2$ for the transition operators. In addition, we choose to always work in the EIT regime characterized by $\Delta_p = \Delta_c = 0$, though the coupling field with $\Omega_c = 5.0 \times 2\pi$ MHz will be adiabatically turned off (on) at $t_1 = 2.5\,\mu$s ($t_2 = 3.5\,\mu$s). In this case, each SA contains on average $n_{SA} \simeq 295$ ($\sim$700) atoms with the blockade radius $R_b \simeq 5\,\mu$m ($12\,\mu$m) when the coupling field is on (off). A dephasing rate γ_s and a frequency shift δ_s (both estimated as a few tens of kilohertz) arising from the vdW interactions between different SAs [44,45] will also be included in our calculations.

We first check in Fig. 2 how the light intensity, the two-photon correlation, the atomic spin field, and the SA Rydberg population evolve during the storage-retrieval process in a Rydberg-EIT medium for a weak probe pulse prepared in the coherent state. It is clear that these four quantities are tightly coupled and propagate together at a slow group velocity of $v_g \approx 240$ m/s when the coupling field is on. This indicates the formation of a Rydberg dark-state polariton (RDP) defined here by $\Psi(z,t) = \cos\theta(z,t)\Omega_p(z,t) - \sin\theta(z,t)S(z,t)$ with $\tan\theta(z,t) = g\sqrt{N[1 - \Sigma_{RR}(z,t)]}/\Omega_c(t)$. When the coupling field is off, the probe field is completely mapped onto the spin field so that the RDP becomes stationary with $v_g = 0$. The above findings are *trivial* because they are typically found when we study light storage and retrieval in cold atoms without a Rydberg state. Two *nontrivial* findings are given below.

First, the light intensity, two-photon correlation and spin field suffer severe dissipation before the coupling field is turned off, while they experience little change after the coupling field is turned on. This is because the two-level polarization P_2 plays a significant (immaterial) role in the presence of a remarkable (negligible) SA Rydberg population in the first (second) stage. Second, the losses in light intensity, two-photon correlation, and spin field are temporally (spatially) inhomogeneous because the Rydberg excitation depends critically on local intensity and correlation of the probe pulse. This can be understood by examining Eq. (5), which indicates that Σ_{RR} will attain higher (lower) values when $n_{SA}|\Omega_p|^2 g_p^{(2)}$ is comparable to (much smaller than) $|\Omega_c|^2$ close to (far away from) the probe pulse center. Note also that a SA Rydberg population

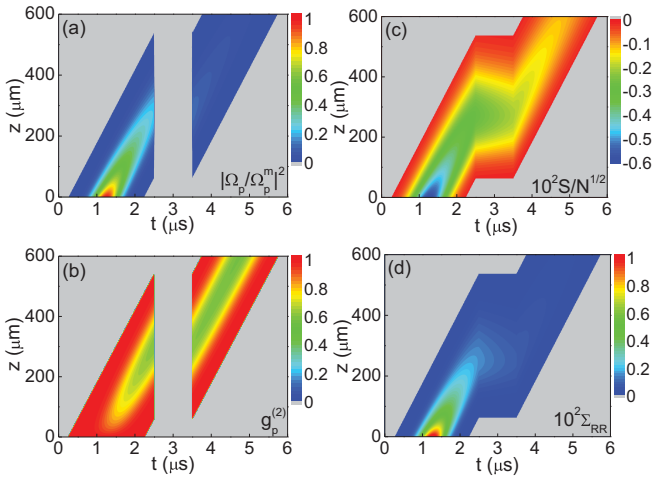

FIG. 2. Dynamic evolution of the scaled light intensity (a), the two-photon correlation (b), the atomic spin field (c), and the SA Rydberg population (d) for an input probe pulse in the coherent state described by $\Omega_p(0,t) = \Omega_p^m e^{-(t-t_0)^2/\delta t^2}$ and $g_p^{(2)}(0,t) = 1.0$. Relevant parameters are given at the beginning of Sec. III, except $\Omega_p^m/2\pi = 0.03$ MHz, $t_0 = 1.25\,\mu$s, and $\delta t = 0.5\,\mu$s.

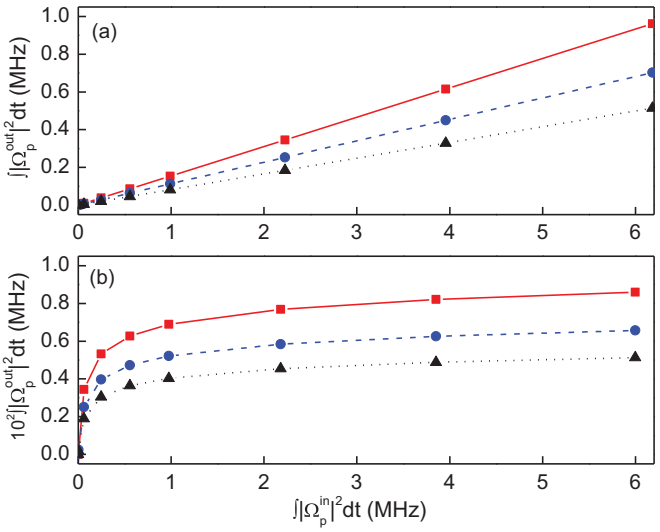

FIG. 4. Output field energy versus input field energy in the absence (a) or presence (b) of a vdW interaction. The red-solid, blue-dashed, and black-dotted curves correspond to storage times of 0.0 μs, 0.5 μs, and 1.0 μs, respectively. Other parameters are the same as in Fig. 2, except $\Omega_p^m/2\pi$ is increased from zero until 0.5 MHz.

$\Sigma_{RR} \simeq 0.01$ is already enough to result in an obvious blockade effect because each SA contains several hundreds of cold atoms for a relatively high atomic density.

Then we compare the input and output probe fields by plotting in Fig. 3 the intensity profile and the two-photon correlation as a function of time. Figure 3(a) shows that the output probe field is greatly attenuated as compared to the input probe field, yet without exhibiting an evident temporal broadening (from 1.85 to 1.89 μs in FWHM). On the contrary, a severe intensity attenuation is typically accompanied by a large temporal broadening for a weak pulse slowly propagating in the usual EIT media. This indicates that the linear absorption

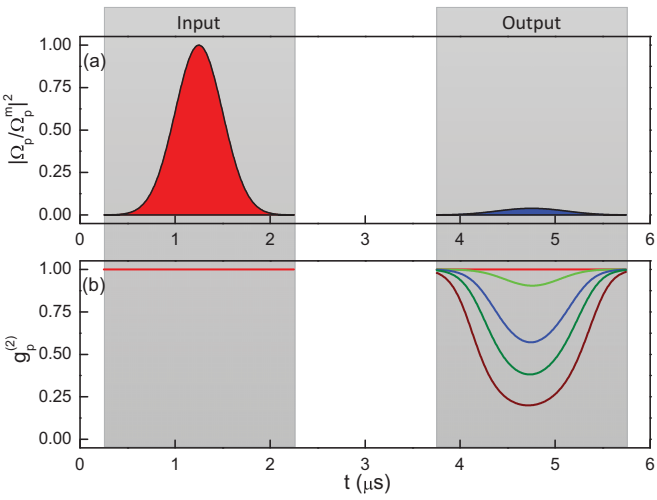

FIG. 3. Intensity profile (a) and two-photon correlation (b) of a quantum probe field at the sample entrance (left) and exit (right) as a function of time. Relevant parameters are the same as in Fig. 2, except $\Omega_p^m/2\pi = 0.001$ MHz, 0.01 MHz, 0.03 MHz, 0.05 MHz, and 0.1 MHz for the five curves in the lower-right panel from top to bottom.

contributed by P_3 of weight $1 - \Sigma_{RR}$ and the nonlinear absorption contributed by P_2 of weight Σ_{RR} are roughly comparable to result in a balanced effect on the probe frequencies at both wings and those at the center of the EIT window. That is, the probe field loses its sideband (central) frequencies mainly due to the linear (nonlinear) absorption. Figure 3(b) shows that the modification of photonic statistics becomes evident for a probe pulse with its maximal amplitude as low as $\Omega_p^m = 0.01$ MHz, and the inhomogeneous two-photon correlation exhibits a stronger and stronger antibunching effect at the pulse center as Ω_p^m is gradually increased. This is consistent with relevant results in Ref. [23], where the modification of two-photon correlation is shown to depend on the input intensity of a cw probe field. Note, however, that square probe pulses may be adopted to attain a homogeneous modification of two-photon correlation and thus a bunch of single photons with $g_p^{(2)} \to 1$.

Now we further calculate in Fig. 4 the output field energy $I_p^{\rm out} = \int|\hat{\Omega}_p(L,t)|^2 dt$ versus the input field energy $I_p^{\rm in} = \int|\hat{\Omega}_p(0,t)|^2 dt$ to verify that there is a restriction on the maximal number of stored probe photons. Figure 4(a) displays that $I_p^{\rm out}$ varies linearly with the increase of $I_p^{\rm in}$ in the absence of a vdW interaction; about 15.5%, 11.4%, and 8.3% probe photons survive at the sample exit due to the linear absorption contributed only by P_3 for storage times of 0.0, 0.5, and 1.0 μs, respectively. Figure 4(b) displays that $I_p^{\rm out}$ varies in a nonlinear way as $I_p^{\rm in}$ is increased in the presence of a vdW interaction; saturation values of 0.14%, 0.11%, and 0.086% survived probe photons are found for storage times of 0.0 , 0.5, and 1.0 μs, respectively. This nonlinear behavior arises as a direct result of Rydberg blockade and is qualitatively consistent with the experimental results in Fig. 1(e) of Ref. [33], where a nonlinear saturation dependence of the output photon number on the input photon number is observed after a partial storage

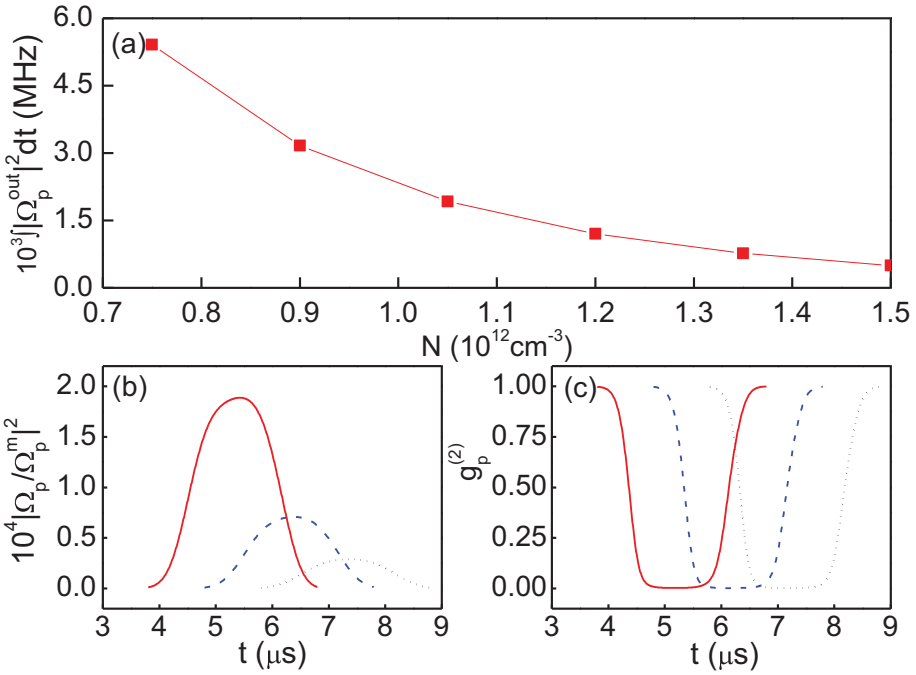

FIG. 5. (a) Saturation value of output field energy versus atomic density. (b) Intensity profile and (c) two-photon correlation of output field as a function of time for $N = 0.9 \times 10^{12}$ cm^{-3} (red-solid), $N = 1.2 \times 10^{12}$ cm^{-3} (blue-dashed), and $N = 1.5 \times 10^{12}$ cm^{-3} (black-dotted). Other parameters are the same as in Fig. 2, except suitable values of $\Omega_p^m/2\pi$ are chosen to attain the saturation effect.

of the probe pulse with a lower atomic density, $N = 3.2 \times 10^{10}$ cm^{-3}. That is, as the input field energy increases, each SA has a larger probability to exhibit one Rydberg excitation so that the traveling probe photons suffer more nonlinear absorption. This is why the same increase of input field energy leads to less and less increase of output field energy until the stored photon number reaches a saturation value. In other words, the number of stored photons is rigidly restricted by the number of SAs in a Rydberg-EIT medium. Note also that as the storage time increases, the saturation value of the output field energy decreases, mainly due to the dephasing rate γ_s.

Finally, we examine in Fig. 5 how the saturation value of output field energy depends on the atomic density. A naive intuition is that this saturation value should be independent of the atomic density because the maximal number of stored photons is determined only by the number of SAs. Figure 5(a) shows, however, that this saturation value reduces quickly as the atomic density is increased. One main reason is that the Rydberg dephasing rate γ_r is not exactly vanishing (especially when the laser linewidth $\delta\omega_2$ is included) so that the linear absorption contributed by P_2 is always perceptible and becomes more evident for a higher atomic density. Consequently, an intermediate density is required to attain a bunch of definite single photons, and more (less) than one photon will be found in a blockade volume for a lower (higher) density. Figures 5(b) and 5(c) show the amplitude profile and the two-photon correlation at the sample exit for three atomic densities. It is clear that the amplitude profile evidently decreases with the increase of the atomic density, whereas the two-photon correlation suffers little change. This indicates that the retrieved field exhibits almost the same photonic statistics, although quenched to different degrees, for different atomic densities. It is worth stressing that the two-photon correlation of an output pulse becomes more homogenous in a dense enough medium.

IV. CONCLUSIONS

In summary, we have studied the storage and retrieval of a multiphoton probe pulse in cold Rydberg atoms driven into the EIT configuration. By developing the SA model to simulate relevant propagation dynamics, we find a few interesting results absent for the light storage and retrieval in usual EIT media. We find in particular that, in the presence of a vdW interaction, (i) the output probe field is greatly attenuated in intensity without suffering an evident temporal broadening due to the roughly balanced linear and nonlinear absorptions; (ii) the output two-photon correlation exhibits a temporally inhomogeneous antibunching feature as the probe field is not too weak and the atomic sample is not too dense; (iii) the output field energy displays a nonlinear saturation value with regard to the input field energy, depending on the atomic density and the storage time. These are all based on the Rydberg blockade effect, which sets a limit for the maximal number of stored and retrieved photons and triggers the interplay of a two-level polarization P_2 and a three-level polarization P_3. A suitable extension of our results could be explored to prepare various nonclassical light fields and manipulate their nonlinear interactions for quantum information applications.

ACKNOWLEDGMENTS

This work is supported by the National Natural Science Foundation of China (Grants No. 11534002, No. 11547261, No. 11674049, and No. 11704063), the Collaborative

Research Project by the Italian Ministry of Foreign Affairs and International Cooperation (Grant No. PGR00960) and the National Natural Science Foundation of China (Grant No. 11861131001), the Graduate Innovation Fund of Jilin University (Grant No. 2016064), the Youth Fund of Liaoning University (Grant No. LDQN201430), and the General Science and Technology Research Plans of Liaoning Educational Bureau (Grant No. L2014002).

[1] M. Saffman, T. G. Walker, and K. Mølmer, Rev. Mod. Phys. **82**, 2313 (2010).
[2] M. D. Lukin, M. Fleischhauer, R. Côté, L. M. Duan, D. Jaksch, J. I. Cirac, and P. Zoller, Phys. Rev. Lett. **87**, 037901 (2001).
[3] D. Tong, S. M. Farooqi, J. Stanojevic, S. Krishnan, Y. P. Zhang, R. Côté, E. E. Eyler, and P. L. Gould, Phys. Rev. Lett. **93**, 063001 (2004).
[4] K. Singer, M. Reetz-Lamour, T. Amthor, L. G. Marcassa, and M. Weidemüller, Phys. Rev. Lett. **93**, 163001 (2004).
[5] E. Urban, T. A. Johnson, T. Henage, L. Isenhower, D. D. Yavuz, T. G. Walker, and M. Saffman, Nat. Phys. **5**, 110 (2009).
[6] A. Gaëtan, Y. Miroshnychenko, T. Wilk, A. Chotia, M. Viteau, D. Comparat, P. Pillet, A. Browaeys, and P. Grangier, Nat. Phys. **5**, 115 (2009).
[7] D. Møller, L. B. Madsen, and K. Mølmer, Phys. Rev. Lett. **100**, 170504 (2008).
[8] D. D. B. Rao and K. Mølmer, Phys. Rev. A **90**, 062319 (2014).
[9] D. D. B. Rao and K. Mølmer, Phys. Rev. Lett. **111**, 033606 (2013).
[10] X.-D. Tian, Y.-M. Liu, C.-L. Cui, and J.-H. Wu, Phys. Rev. A **92**, 063411 (2015).
[11] I. I. Beterov, M. Saffman, E. A. Yakshina, V. P. Zhukov, D. B. Tretyakov, V. M. Entin, I. I. Ryabtsev, C. W. Mansell, C. MacCormick, S. Bergamini, and M. P. Fedoruk, Phys. Rev. A **88**, 010303 (2013).
[12] M. M. Müller, M. Murphy, S. Montangero, T. Calarco, P. Grangier, and A. Browaeys, Phys. Rev. A **89**, 032334 (2014).
[13] D. Petrosyan, F. Motzoi, M. Saffman, and K. Mølmer, Phys. Rev. A **96**, 042306 (2017).
[14] M. H. Goerz, E. J. Halperin, J. M. Aytac, C. P. Koch, and K. B. Whaley, Phys. Rev. A **90**, 032329 (2014).
[15] H.-Z. Wu, X.-R. Huang, C.-S. Hu, Z.-B. Yang, and S.-B. Zheng, Phys. Rev. A **96**, 022321 (2017).
[16] Y. O. Dudin and A. Kuzmich, Science **336**, 887 (2012).
[17] D. Petrosyan, D. D. B. Rao, and K. Mølmer, Phys. Rev. A **91**, 043402 (2015).
[18] C. Tresp, C. Zimmer, I. Mirgorodskiy, H. Gorniaczyk, A. Paris-Mandoki, and S. Hofferberth, Phys. Rev. Lett. **117**, 223001 (2016).
[19] S. Baur, D. Tiarks, G. Rempe, and S. Durr, Phys. Rev. Lett. **112**, 073901 (2014).
[20] W. Li and I. Lesanovsky, Phys. Rev. A **92**, 043828 (2015).
[21] H. Gorniaczyk, C. Tresp, J. Schmidt, H. Fedder, and S. Hofferberth, Phys. Rev. Lett. **113**, 053601 (2014).
[22] D. Tiarks, S. Baur, K. Schneider, S. Dürr, and G. Rempe, Phys. Rev. Lett. **113**, 053602 (2014).
[23] D. Petrosyan, J. Otterbach, and M. Fleischhauer, Phys. Rev. Lett. **107**, 213601 (2011).
[24] J. D. Pritchard, D. Maxwell, A. Gauguet, K. J. Weatherill, M. P. A. Jones, and C. S. Adams, Phys. Rev. Lett. **105**, 193603 (2010).
[25] T. Peyronel, O. Firstenberg, Q.-Y. Liang, S. Hofferberth, A. V. Gorshkov, T. Pohl, M. D. Lukin, and V. Vuletić, Nature (London) **488**, 57 (2012).
[26] Y.-M. Liu, D. Yan, X.-D. Tian, C.-L. Cui, and J.-H. Wu, Phys. Rev. A **89**, 033839 (2014).
[27] W. Li, D. Viscor, S. Hofferberth, and I. Lesanovsky, Phys. Rev. Lett. **112**, 243601 (2014).
[28] P. Bienias, S. Choi, O. Firstenberg, M. F. Maghrebi, M. Gullans, M. D. Lukin, A. V. Gorshkov, and H. P. Büchler, Phys. Rev. A **90**, 053804 (2014).
[29] M. F. Maghrebi, M. J. Gullans, P. Bienias, S. Choi, I. Martin, O. Firstenberg, M. D. Lukin, H. P. Büchler, and A. V. Gorshkov, Phys. Rev. Lett. **115**, 123601 (2015).
[30] M. Moos, R. Unanyan, and M. Fleischhauer, Phys. Rev. A **96**, 023853 (2017).
[31] S. Sevincli, N. Henkel, C. Ates, and T. Pohl, Phys. Rev. Lett. **107**, 153001 (2011).
[32] Y.-M. Liu, X.-D. Tian, X. Wang, D. Yan, and J.-H. Wu, Opt. Lett. **41**, 408 (2016).
[33] E. Distante, A. Padrón-Brito, M. Cristiani, D. Paredes-Barato, and H. de Riedmatten, Phys. Rev. Lett. **117**, 113001 (2016).
[34] D. Maxwell, D. J. Szwer, D. Paredes-Barato, H. Busche, J. D. Pritchard, A. Gauguet, K. J. Weatherill, M. P. A. Jones, and C. S. Adams, Phys. Rev. Lett. **110**, 103001 (2013).
[35] I. Mirgorodskiy, F. Christaller, C. Braun, A. Paris-Mandoki, C. Tresp, and S. Hofferberth, Phys. Rev. A **96**, 011402(R) (2017).
[36] F. Ripka, Y.-H. Chen, R. Löw, and T. Pfau, Phys. Rev. A **93**, 053429 (2016).
[37] J. Ruseckas, I. A. Yu, and G. Juzeliūnas, Phys. Rev. A **95**, 023807 (2017).
[38] A. V. Gorshkov, R. Nath, and T. Pohl, Phys. Rev. Lett. **110**, 153601 (2013).
[39] M. J. Gullans, J. D. Thompson, Y. Wang, Q.-Y. Liang, V. Vuletić, M. D. Lukin, and A. V. Gorshkov, Phys. Rev. Lett. **117**, 113601 (2016).
[40] M. Moos, M. Höning, R. Unanyan, and M. Fleischhauer, Phys. Rev. A **92**, 053846 (2015).
[41] L. Yang, B. He, J.-H. Wu, Z.-Y. Zhang, and M. Xiao, Optica **3**, 1095 (2016).
[42] E. Zeuthen, M. J. Gullans, M. F. Maghrebi, and A. V. Gorshkov, Phys. Rev. Lett. **119**, 043602 (2017).
[43] J.-H. Wu, M. Artoni, F. Cataliotti, and G. C. La Rocca, Europhys. Lett. **120**, 54002 (2017).
[44] M. Garttner, S. Whitlock, D. W. Schonleber, and J. Evers, Phys. Rev. A **89**, 063407 (2014).
[45] J.-S. Han, T. Vogt, and W.-H. Li, Phys. Rev. A **94**, 043806 (2016).